LETTERS

The *Ter* mutation in the dead end gene causes germ cell loss and testicular germ cell tumours

Kirsten K. Youngren[1], Douglas Coveney[3], Xiaoning Peng[4], Chitralekha Bhattacharya[4], Laura S. Schmidt[5], Michael L. Nickerson[6], Bruce T. Lamb[1], Jian Min Deng[4], Richard R. Behringer[4], Blanche Capel[3], Edward M. Rubin[7], Joseph H. Nadeau[1,2] & Angabin Matin[4]

In mice, the *Ter* mutation causes primordial germ cell (PGC) loss in all genetic backgrounds[1]. *Ter* is also a potent modifier of spontaneous testicular germ cell tumour (TGCT) susceptibility in the 129 family of inbred strains, and markedly increases TGCT incidence in 129-*Ter/Ter* males[2–4]. In 129-*Ter/Ter* mice, some of the remaining PGCs transform into undifferentiated pluripotent embryonal carcinoma cells[2–6], and after birth differentiate into various cells and tissues that compose TGCTs. Here, we report the positional cloning of *Ter*, revealing a point mutation that introduces a termination codon in the mouse orthologue (*Dnd1*) of the zebrafish *dead end* (*dnd*) gene. PGC deficiency is corrected both with bacterial artificial chromosomes that contain *Dnd1* and with a *Dnd1*-encoding transgene. *Dnd1* is expressed in fetal gonads during the critical period when TGCTs originate. DND1 has an RNA recognition motif and is most similar to the apobec complementation factor, a component of the cytidine to uridine RNA-editing complex. These results suggest that *Ter* may adversely affect essential aspects of RNA biology during PGC development. DND1 is the first protein known to have an RNA recognition motif directly implicated as a heritable cause of spontaneous tumorigenesis. TGCT development in the 129-*Ter* mouse strain models paediatric TGCT in humans. This work will have important implications for our understanding of the genetic control of TGCT pathogenesis and PGC biology.

Ter was mapped to mouse chromosome 18 near *Fgf1* by following

inheritance of genetic markers and two phenotypes: tumour incidence and PGC deficiency[7,8] (Fig. 1a–c). Testis weight was used as a surrogate quantitative phenotype for *Ter* in high-resolution interspecific and intersubspecific backcrosses and intercrosses (Supplementary Fig. 1). A total of 2,753 meioses were examined from crosses between the B6.129-*Ter* congenic strain and A/J, C57BL/6J, C3H/HeJ and MOLF/Ei strains to avoid recombination 'hot'- and 'cold'-spots that may exist in the genome of particular strains. Genotyping of F_2 progeny with microsatellite markers narrowed the critical interval to 0.14 cM between *273* and *173RB* (Fig. 2a). Four overlapping bacterial artificial chromosomes (BACs) spanned the *Ter* locus: RG-MBAC_173P21, RG-MBAC_282N17, RG-MBAC_273D11 and RG-MBAC_284F9, derived from the 129 strain.

We used BAC complementation tests to reduce further the size of the critical interval. Transgenic mice were generated with each of the four overlapping BACs. They were crossed to B6.129-*Ter* congenic mice to eventually generate *Ter/Ter* mice carrying individual transgenes. Mice with BACs 282N17 and 284F9, but not BACs 273D11 and 173P21, rescued the germ-cell-deficient phenotype (Supplementary Fig. 1), fully or partially restoring fertility in *Ter/Ter* mice, as assessed histologically (Fig. 2c, d) and by breeding performance (not shown), thus demonstrating that the overlapping region between 282N17 and 284F9 harbours *Ter*.

Four genes are present within the overlapping region of BACs
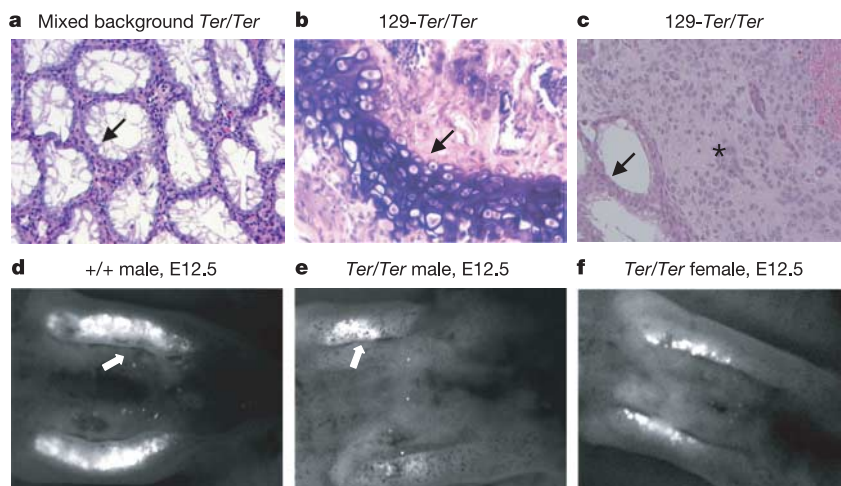
Figure 1 | Gonadal phenotypes of *Ter/Ter* males.
a, Testis of a 4-week-old *Ter/Ter* male showing lack of germ cells (arrow points to Sertoli cell only phenotype) in the seminiferous tubules. **b, c**, Histological sections through TGCTs from 4-week-old 129-*Ter/Ter* male mice. Tissue types observed include cartilage (arrow in **b**) and neuroepithelia (asterisk in **c**). The arrow in **c** indicates germ-cell-deficient seminiferous tubules adjacent to neuroepithelial cells of the tumour. **d–f**, GFP-tagged PGCs. Genital ridges of E12.5 embryos showing GFP expression in PGCs of a 129-+/+;*Oct4*–GFP male (**d**), 129-*Ter/Ter*;*Oct4*–GFP male (**e**) and 129-*Ter/Ter*;*Oct4*–GFP female (**f**). The arrow indicates one of the genital ridges of the dissected embryo.

a | Mixed background *Ter/Ter*   b | 129-*Ter/Ter*   c | 129-*Ter/Ter*
d | +/+ male, E12.5   e | *Ter/Ter* male, E12.5   f | *Ter/Ter* female, E12.5

[1]Department of Genetics and [2]Case Comprehensive Cancer Center, Case Western Reserve University, Cleveland, Ohio 44106, USA. [3]Department of Cell Biology, Duke University, Durham, North Carolina 27710, USA. [4]Department of Molecular Genetics, University of Texas, MD Anderson Cancer Center, Houston, Texas 77030, USA. [5]Basic Research Program, SAIC-Frederick, Inc., and [6]Laboratory of Immunobiology, NCI Frederick, Frederick, Maryland 21702, USA. [7]Genome Sciences Department, Lawrence Berkeley National Laboratory, Berkeley, California 94720, USA.

282N17 and 284F9 (Fig. 2b). Comparison of the sequences of all the exons of these four genes from 129-*Ter*/*Ter* and 129-+/+ mice revealed a single base change (C to T) in the coding region of the *Dnd1* gene (Fig. 3a, b), which is the orthologue of zebrafish *dnd*[9]. This substitution introduces a stop codon (R178X) in the coding regions of both isoforms of mouse *Dnd1*-encoded protein (DND1) at amino acids 178 and 190, respectively (Fig. 3a; accession numbers BC034897 and AY321066, NCBI). The mutation was found only in mice carrying *Ter*, but not in 129 substrains (129T2/SvEmsJ, 129S1/SvImJ, 129X1/SvJ) or other inbred strains (A/J, C57BL/6J, C3H/HeJ and MOLF/Ei). The base change introduces a new *Dde*1 restriction enzyme site within the *Dnd1* sequence, enabling mice with the *Ter* allele to be distinguished from wild-type mice (Supplementary Fig. 1).

To confirm that *Ter* is due to mutation in *Dnd1*, we used a 3.9-kilobase (kb) genomic DNA fragment derived from BAC 284F9 that encodes only the *Dnd1* gene plus 860 base pairs (bp) and 510 bp flanking 5′ and 3′ ends, respectively, as a transgene (*Tg(Dnd1)1Matn*) to rescue the *Ter*/*Ter* phenotype. *Ter*/*Ter* males positive for *Tg(Dnd1)1Matn* showed partial rescue of the germ-cell-deficient phenotype (Fig. 2e). Although many seminiferous tubules remained germ-cell-deficient, some contained immature and mature sperm, which is unprecedented in *Ter*/*Ter* males.

Double-stranded RNAs, which can result from expression of overlapping genes on opposite strands, can lead to loss of messenger RNA or translational silencing[10,11]. *Dnd1* and *Wdr55* (2410080P20Rik) are encoded on opposite strands of DNA and overlap by 35 bp in the 3′ ends of their last exon (Fig. 2b). To test whether the mutation impairs function of *Wdr55* and indirectly leads to the *Ter* phenotype, we created mice with targeted deletion of *Wdr55* (*wdr55*^tm1Matn) (Supplementary Fig. 2). Mice homozygous for *wdr55*^tm1Matn are embryonic lethal and die before embryonic day

(E)9.5. In contrast, *Ter*/*Ter* mice are viable but sterile. Moreover, double heterozygote males (+ *wdr55*^tm1Matn/*Ter* +) were not germ-cell-deficient and had gonad/body mass ratios ranging from 3.3 to 4.1, which is typical of wild-type but not *Ter*/*Ter* mice. Thus, *Ter* is not an allele of *Wdr55*. Therefore, functional complementation of *Tg(Dnd1)1Matn* transgenic mice together with normal testes in double heterozygotes demonstrates that the mutation in *Dnd1* directly causes the *Ter* phenotype.

Expression of *Dnd1*^Ter was characterized by northern and western blotting analyses. Northern analysis revealed that transcripts of both *Dnd1* isoforms are expressed in adult testes but only one isoform in adult heart (Fig. 3c). *Dnd1* transcripts were significantly decreased in tumours from 129-*Ter*/*Ter* males (Fig. 3d). Transcript levels of the other genes in the critical interval (*Wdr55*, *Ik* and *Ndufa2*) were also reduced to varying extents in tumour tissue, suggesting that these genes also function in normal adult testes. The two DND1 protein isoforms differ at the first 33 and 45 amino acids of their respective amino terminus. A polyclonal antibody was generated against an 18-amino-acid peptide of one isoform of DND1 (indicated by A in Fig. 3a). Western blotting of lysates from normal testes revealed a protein of 38 kDa, which is nearly the expected size (37.5 kDa) of the DND1 protein (Supplementary Fig. 1). This antibody also recognized a 62.5-kDa glutathione *S*-transferase (GST)–DND1 fusion protein. DND1 was not detected in protein lysates from germ-cell-deficient testes of three different B6.129-*Ter*/*Ter* males or from tumours of four different 129-*Ter*/*Ter* males (Fig. 3e). Thus, the various cell types of the tumours do not retain DND1 expression. However, a truncated DND1 protein was also not detected in *Ter*/*Ter* tumours. This rules out the possibility that tumour development is due to a dominant-negative-acting, oncogenic truncated DND1 protein. We note that the antibody we used detects only one isoform of DND1, and cannot rule out the possibility that the other isoform is
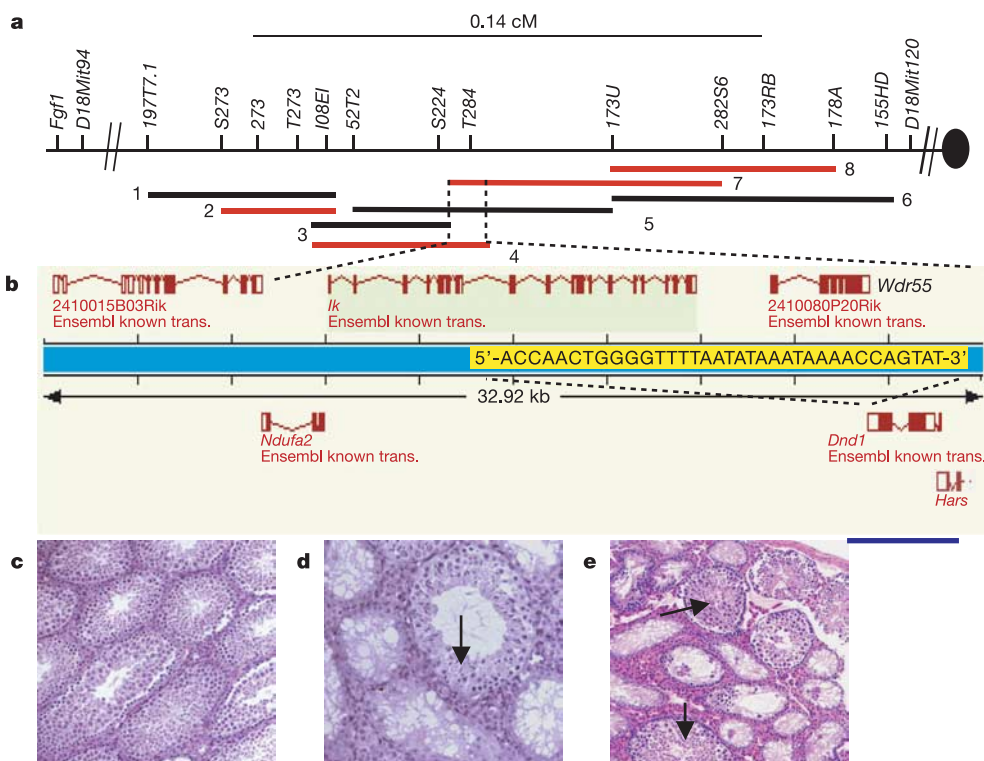
Figure 2 | Positional cloning of *Ter*. a, Physical map of the *Ter* locus. The 129-derived (RG-MBAC) BAC contig: 1 = 197J23, 2 = 173P21, 3 = 224K2, 4 = 284F9, 5 = 52N10, 6 = 368A6, 7 = 282N17, 8 = 273D11. **b**, Ensembl gene map of the overlapping region of BACs 284F9 and 282N17. Overlapping bases of the last exons of *Wdr55* and *Dnd1* are marked in yellow. The blue line indicates the DNA fragment used in *Tg(Dnd1)1Matn*. **c, d**, Testes histology of a *Ter*/*Ter* mouse with BAC 284F9 (**c**) and a sibling also with the transgene (**d**) where rescue occurs in a subset of seminiferous tubules (arrow). **e**, Histology of *Ter*/*Ter* testes with *Tg(Dnd1)1Matn* (the arrow shows a normal seminiferous tubule).

still expressed. However, that seems to be unlikely because the mutation introduces a stop codon in both isoforms of DND1.

129-*Ter*/+ mice have a modestly elevated TGCT incidence, with 17% of the males having a unilateral tumour[2]. To test how *Dnd1* is involved in tumour development in heterozygous males, we obtained testicular tumours and contralateral normal testes from two 129-*Ter*/+ mice, and bisected each of these tissues to examine *Dnd1* protein and RNA expression. DND1 was not detected in tumour protein lysates (Fig. 3f), although the contralateral normal testes of the 129-*Ter*/+ mice expressed DND1. To determine the mechanism of protein loss, we examined RNA from the 129-*Ter*/+ tumour samples. Because the tumour sizes were typically small, we used polymerase chain reaction with reverse transcription (RT–PCR) to amplify the full-length *Dnd1* complementary DNA, and detected both the normal wild-type and mutated transcripts from tumour tissues via sequencing. We then developed an RT–PCR-based assay (see Methods) to distinguish visually mRNA from the normal (+) and the *Dnd1*[Ter] allele (Fig. 3g, left). Using this method, the wild-type transcript was observed in tumours as well as in normal testes (Fig. 3g, right). Because RT–PCR is a sensitive technique we were also able to amplify the *Dnd1*[Ter] transcript (Fig. 3g, labelled m) from the *Ter*/+ RNA. However, the *Dnd1*[Ter] transcript band is weaker compared with the wild-type allele. Taking into consideration both the western (Fig. 3f) and RT–PCR data (Fig. 3g, left), it indicates that

inactivation of DND1 expression from the wild-type allele of 129-*Ter*/+ (a second 'hit') has resulted in tumour development. In the case of the two samples examined, the second hit is probably a post-transcriptional mechanism such as translational silencing[12,13].

The defect that underlies PGC deficiency and TGCT susceptibility in *Ter* males occurs during embryogenesis[1]. We therefore examined normal embryonic expression of *Dnd1* and detected it at earlier stages than reported previously[9]. Whole-mount *in situ* hybridization using a *Dnd1*-specific RNA probe detected expression in the embryo and allantoic bud at E7.5, neuroectoderm at E8.5, and widespread expression in E9.5 embryo including the neural tube, head mesenchyme, first branchial arch and the hindgut, through which primordial germ cells are migrating (Supplementary Fig. 3). *Dnd1* expression was also detected in the XY and XX genital ridges of E11.5 embryos (Fig. 4a, b). *Dnd1* expression was upregulated in the testis cords of the XY gonad between E12.5 and E14.5 (Figs 4c, e), but downregulated between E12.5 and E14.5 in XX gonads (Fig. 4d, f). Downregulation of *Dnd1* in the XX gonad occurred progressively from anterior to posterior, similar to the wave of meiotic entry of XX germ cells[14,15]. The contrasting patterns of *Dnd1* expression in XX versus XY gonads may account for the differential susceptibility to teratocarcinogenesis in female versus male 129-*Ter*/*Ter* mice.

To visualize PGCs in 129-*Ter*/*Ter* embryos, we introduced a green
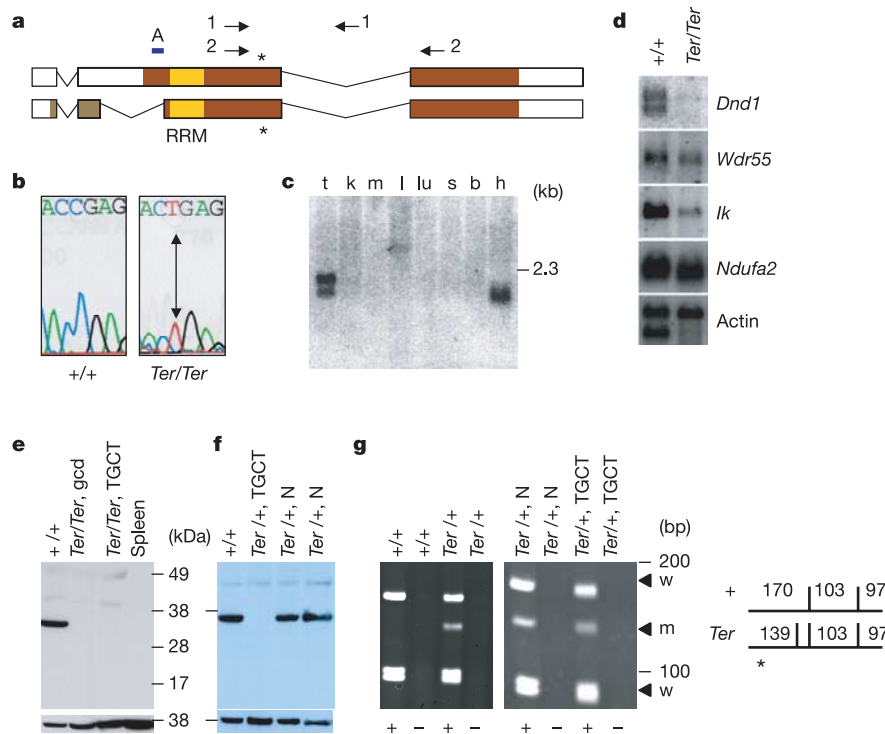
Figure 3 | Expression of *Dnd1* in normal tissues and TGCTs. a, Comparison of DND1 isoforms with accession numbers BC034897 (top) and AY321066 (bottom). Coloured regions indicate protein-coding regions; yellow box marks an RNA recognition motif. An asterisk indicates amino acids 178 and 190, of the two isoforms, which are mutated (R178X) in *Ter*. Arrows indicate primers 4.13a (1) and A25 (2). A indicates the region used as peptide epitope to generate anti-DND1 antibody. **b**, C to T mutation in *Ter*/*Ter* introduces a stop codon. **c**, Mouse tissue northern blot for *Dnd1*. mRNAs are from testes (t), kidney (k), muscle (m), liver (l), lung (lu), spleen (s), brain (b) and heart (h). **d**, Northern blot of mRNA from 129-+/+ testes and 129-*Ter*/*Ter* tumours. **e**, Western blot with anti-DND1 antibody of tissue lysates from normal (+/+) testes of a 129-+/+ mouse, germ-cell-deficient (gcd) testes of a B6.129-*Ter*/*Ter* congenic strain, bilateral TGCTs from a 129-*Ter*/*Ter* mouse, and spleen of a 129-+/+ mouse. The bottom panel shows control for loading

using anti-β-actin. **f**, Western blot with anti-DND1 of normal testes of a 129-+/+ mouse, tumour in the testes of a 129-*Ter*/+ (*Ter*/+, TGCT) mouse, the normal contralateral testes (*Ter*/+, N) and normal testes of another 129-*Ter*/+ mouse (*Ter*/+, N). The bottom panel shows the same blot re-hybridized with mouse anti-β-actin. **g**, RT–PCR of RNA from normal testes of 129-+/+ and 129-*Ter*/+ mice using the A25 primer (2 in panel **a**) followed by *Dde*1 digestion (left panel). This produces fragments of 170, 103 and 97 bp from the wild-type allele and 139, 103, 97 and 31 bp (not seen on gel) from the *Ter* allele. For controls, PCR reactions were performed on samples that included (+) or did not include (−) Superscript II during RT, as indicated below the panels. The right panel shows total RNA from normal and TGCT-bearing testes of the same 129-*Ter*/+ mouse, amplified by RT–PCR followed by *Dde*1 digestion and electrophoresis. The arrows indicate the wild-type (w) and *Ter* (m) allele.

fluorescent protein (GFP) transgene driven by the PGC-specific Oct4 promoter[16] (*GOF-1/ΔPE/EGFP*) in the 129-*Ter* strain. At E12.5, the number of GFP-labelled PGCs was significantly reduced in the urogenital ridges of 129-*Ter/Ter* compared with 129-+/+ embryos (Fig. 1d–f). However, the few surviving PGCs in *Ter/Ter* embryos had successfully migrated to the genital ridges[1], and tumours eventually occur in the testes of *Ter/Ter* mice. Therefore, *Dnd1* is not essential for PGC migration in the mouse. Loss of PGCs in 129-*Ter/Ter* embryos precedes development of embryonal carcinoma cells and TGCTs. Inactivation of *Dnd1* expression in PGCs during embryogenesis in 129-*Ter/Ter* mice is therefore implicated as the causal event that drives PGCs to exit the germ line and transform to embryonal carcinoma cells and TGCTs.

The mouse DND1 protein shares sequence similarity with proteins with RNA recognition motifs, with highest similarity to mouse apobec complementation factor (Acf, XP_129159; 34% overall amino acid identity and 48% identity in the RNA recognition motif) (Supplementary Fig. 4). *Acf* encodes the RNA-binding subunit of the RNA-editing enzyme complex (editosome) that converts specific cytidines to uridines in the apolipoprotein B transcript and other RNAs[17]. Several RNA-binding proteins are anomalously expressed in certain cancers[18–23], but it is unclear whether these are causes or consequences of tumorigenesis. DND1 may be an RNA- or DNA-binding subunit of other apobec-like proteins[24] involved in nucleic-acid editing, and the *Ter* mutation raises the possibility that TGCT susceptibility is a consequence of aberrant nucleic acid editing.

Various aspects of RNA biology have central roles in the development of the PGC lineage[25–27]. We show that functional inactivation of the mouse *Dnd1* gene results in severe germ cell deficiency and increased TGCT susceptibility. Our findings implicate a causal role of RNA biology in TGCT susceptibility, as DND1 has an RRM motif[28] and is most similar to Acf, which is involved in RNA editing. Extrapolating from the findings in *Ter* mice, although germ cell tumours present clinically in infants and young adults, it is apparent that genetic and environmental influences during embryogenesis increase the susceptibility of PGCs to tumorigenesis. 129-*Ter* mice are a valuable model system to study the initiating events of tumorigenesis, because the cell of origin of the tumours and the time of onset is defined, and now one of the defects (the *Ter* mutation in *Dnd1*) that predisposes to PGC transformation has been identified.

Figure 4 | Expression of *Dnd1* in embryonic gonads. a, **b**, Whole-mount *in situ* hybridization of E11.5 XY (**a**) and E11.5 XX (**b**) genital ridge (g) and mesonephros (m), in which *Dnd1* expression is localized to the gonad. **c**, **d**, Whole-mount *in situ* hybridization of an E12.5 XY (**c**) gonad (t), in which *Dnd1* is localized to testis cords (tc), whereas *Dnd1* expression in an E12.5 XX (**d**) gonad (o) has a broad distribution throughout the gonad. **e**, **f**, Whole-mount *in situ* hybridization of an E14.5 XY (**f**) gonad, in which *Dnd1* is localized to testis cords, in contrast to E14.5 XX (**f**) gonads, in which *Dnd1* expression is reduced. **g** and **h** show section *in situ* hybridization of an E12.5 XY and E13.5 XY gonad, respectively. *Dnd1* is specific to developing testicular cords in the E12.5 and E13.5 XY gonads. Scale bars represent 500 μm.
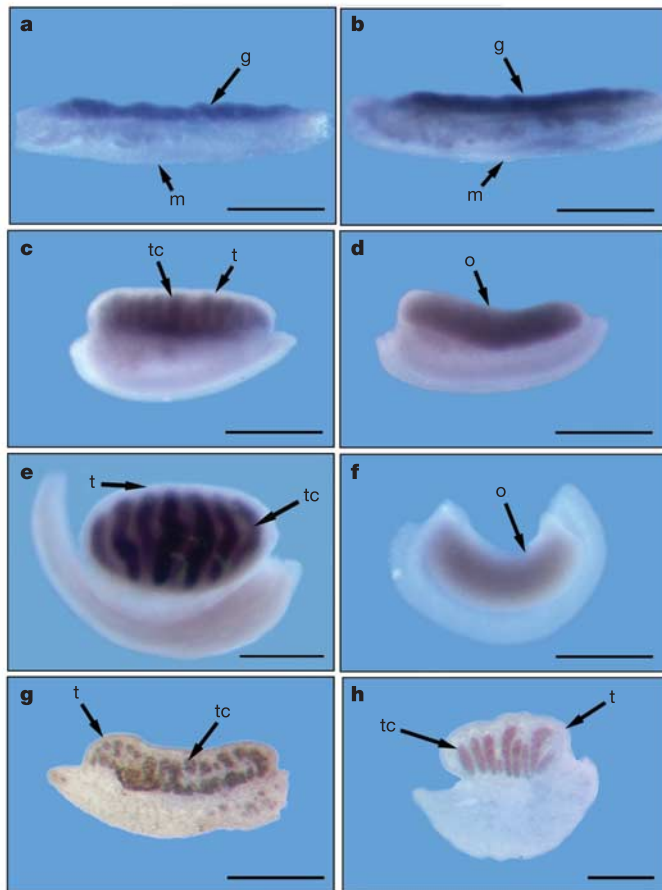
METHODS

Nomenclature. The orthologue of *Ter* in zebrafish is the *dead end* (*dnd*) gene[9]. On the basis of orthology with *dnd*, we call the mouse gene dead end, with gene and allele symbol *Dnd1* and *Dnd1^Ter^*, respectively. Mouse *Dnd1* accession numbers are BC034897 and AY321066 (NCBI). The gene 2410080P20Rik (NM_026464) on the opposite strand and partially overlapping with *Dnd1* was named *Wdr55*. Accession numbers for *Ik* and *Ndufa2* are NM_011879 and NM_010885, respectively.

Generation of genetic and physical maps. Polymorphic microsatellites were subcloned from the BACs using colony hybridization and mapped to chromosome 18 (primers to amplify the polymorphic markers are listed in Supplementary Fig. 4). Accession numbers of the BACs are: AC027276 for RG-MBAC_173P21, AC027278 for RG-MBAC_284F9, AC087795 for RP23-181H5 (which is the C57BL/6J equivalent of RG-MBAC_282N17) and AC087772 for RP23-326L17 (which is the C57BL/6J equivalent of RG-MBAC_2849F). BAC RG-MBAC_273D11 was not sequenced.

Creation of BAC and *Tg(Dnd1)1Am* transgenics. BACs were purified, linearized and microinjected into FVB fertilized one-cell embryos[29]. PCR analysis to test for the presence of the BAC transgenes was carried out using the primers BAC-51-F 5′-CTTAACTATGCGGCATCAGAGC-3′ and BAC-201-R 5′-GCCAGCTGGCGTAATAGCGAAG-3′, which amplified a 173-bp fragment from the vector-insert junction. Mice carrying the 129-derived chromosomal segment spanning *D18Mit232*, *D18Mit94* and *D18Mit17* (*Ter/+*) and mice positive for BAC transgenes were intercrossed. Genotyping for the 129-derived chromosomal segment identified *Ter/Ter* mice bearing individual BAC transgenes. To generate *Tg(Dnd1)1Matn*, BAC 284F9 was digested with *Bgl*II and *Nhe*1 and subcloned into pBlueScript II KS+. The 3.9-kb fragment encoding *Dnd1* was identified by hybridization with ³²P-labelled PCR product of primers 4.13a-F and 4.13a-R (Supplementary Methods). The 3.9-kb fragment was purified, linearized and microinjected into FVB-fertilized one-cell embryos. Primers designed against the vector-insert boundary, A16.1-F 5′-GTCATCC TTGCACGCTGCGCACG-3′ and A16.1-R 5′-GCTTGATATCGAATTCCTG-3′, were used for PCR genotyping for the presence of *Tg(Dnd1)1Matn*. Founder mice were crossed to the B6.129-*Ter* congenic strain. Mice carrying the 129-derived chromosomal segment spanning *D18Mit232*, *D18Mit94* and *D18Mit17* (*Ter/+*) and positive for the *Tg(Dnd1)1Matn* transgene were intercrossed to generate *Ter/Ter* mice bearing the *Tg(Dnd1)1Matn* transgene. Testis weight measurements were taken for male progeny and stained sections were examined histologically.

Gonad/body weight ratios and histology. Adult mice (4 weeks of age or older) were killed and the body weight and testis weight recorded. The gonad/body weight ratio was calculated as (gonad weight/body weight) × 1,000. Testes or tumours were preserved in 10% phosphate-buffered formalin for at least 48 h. Sections (5 μm) were stained with haematoxylin and eosin.

In situ hybridization. Embryos and gonads were fixed in 4% PFA for 12 h at 4 °C, washed in 0.1% Tween 20/PBS, dehydrated in 100% methanol and stored at 20 °C until used. Full-length cDNA of *Dnd1* (image clone ID: 3470697) was used as probe. *In situ* hybridizations on mouse embryos were performed as described previously[30].

Generation of anti-DND1 antibody and GST–DND1. Rabbit polyclonal antibody was generated against the DND1 peptide spanning amino acids 16–33. GST–DND1 fusion protein was made by cloning *Dnd1* cDNA in-frame into pGEX-2TK (Amersham Biosciences). GST–DND1 fusion protein was induced by isopropyl-β-D-thiogalactoside and affinity purified using gluta-thione Sepharose 4B.

Assays to distinguish the *Dnd* alleles. To distinguish the mRNA transcripts from the wild-type and *Ter* alleles of *Dnd1*, total RNA from 129-+/+ and 129-*Ter*/+ testes and tumours were treated with DNase1 before converting to cDNA using Superscript II Rnase H Reverse Transcriptase (Invitrogen). PCR was performed using the primers A25-F 5′-CGAGCTGACGGTGGACGGGCTGCC-3′ and A25-R 5′-CTGCCTAGCTTCATCCGTTGAC-3′ (primers 2, Fig. 3a), which were designed to span exons 2 and 3 of *Dnd1* to yield a 396-bp product. The RT–PCR products were digested with *Dde*1 before electrophoresis on a 7% acrylamide gel. *Dde*1 digestion of RT–PCR product produces fragments of 170, 103 and 97 bp from the wild-type allele and 139, 103, 97 and 31 bp from the *Ter* allele. The 31-bp fragment was not observed on the gel (Fig. 3g). Controls to exclude amplification of contaminating DNA were performed on parallel RNA samples by leaving out Superscript II during the reverse transcription reaction (indicated in the lanes marked −). The primers Dnd13-F (5′-CAGGAGCCAG AAAGGTATCAATA-3′) and Dnd13-R (5′-CTTAACCCATTTAGGGTACCTGT-3′) were used to amplify a 1,059-bp *Dnd1* transcript by RT–PCR for sequencing.

1. Sakurai, T., Iguchi, T., Moriwaki, K. & Noguchi, M. The *ter* mutation first causes primordial germ cell deficiency in *ter/ter* mouse embryos at 8 days of gestation. *Dev. Growth Differ.* **37**, 293–302 (1995).
2. Noguchi, T. & Noguchi, M. A recessive mutation (*ter*) causing germ cell deficiency and a high incidence of congenital testicular teratomas in 129/Sv-*ter* mice. *J. Natl. Cancer Inst.* **75**, 385–392 (1985).
3. Stevens, L. C. A new inbred subline of mice (129-terSv) with a high incidence of spontaneous congenital testicular teratomas. *J. Natl Cancer Inst.* **50**, 235–242 (1973).
4. Stevens, L. C. & Mackensen, J. A. Genetic and environmental influences on teratocarcinogenesis in mice. *J. Natl Cancer Inst.* **27**, 443–453 (1961).
5. Stevens, L. C. Origin of testicular teratomas from primordial germ cells in mice. *J. Natl Cancer Inst.* **38**, 549–552 (1967).
6. Donovan, P. J. & de Miguel, M. P. Turning germ cells into stem cells. *Curr. Opin. Genet. Dev.* **13**, 463–471 (2003).
7. Asada, Y., Varnum, D. S., Frankel, W. N. & Nadeau, J. H. A mutation in the *Ter* gene causing increased susceptibility to testicular teratomas maps to mouse chromosome 18. *Nature Genet.* **6**, 363–368 (1994).
8. Sakurai, T., Katoh, H., Moriwaki, K., Noguchi, T. & Noguchi, M. The *ter* primordial germ cell deficiency mutation maps near *Grl-1* on mouse chromosome 18. *Mamm. Genome* **5**, 333–336 (1994).
9. Weidinger, G. *et al. dead end*, a novel germ plasm component, is required for zebrafish primordial germ cell migration and survival. *Curr. Biol.* **13**, 1429–1434 (2003).
10. Mello, C. C. & Conte, D. Revealing the world of RNA interference. *Nature* **431**, 338–342 (2004).
11. Meister, G. & Tuschl, T. Mechanisms of gene silencing by double-stranded RNA. *Nature* **431**, 343–349 (2004).
12. Shao, J., Sheng, H., Inoue, H., Morrow, J. D. & DuBois, R. N. Regulation of constitutive cyclooxygenase-2 expression in colon carcinoma cells. *J. Biol. Chem.* **275**, 33951–33956 (2000).
13. Mukhopadhyay, D., Houchen, C. W., Kennedy, S., Dieckgraefe, B. K. & Anant, S. Coupled mRNA stabilization and translational silencing of cyclooxygenase-2 by a novel RNA binding protein, CUGBP2. *Mol. Cell* **11**, 113–126 (2003).
14. Yao, H. H., DiNapoli, L. & Capel, B. Meiotic germ cells antagonize mesonephric cell migration and testis cord formation in mouse gonads. *Development* **130**, 5895–5902 (2003).
15. Menke, D. B., Koubova, J. & Page, D. C. Sexual differentiation of germ cells in XX mouse gonads occurs in an anterior-to-posterior wave. *Dev. Biol.* **262**, 303–312 (2003).
16. Scholer, H. R., Dressler, G. R., Balling, R., Rohdewohld, H. & Gruss, P. Oct-4: a germline-specific transcription factor mapping to the mouse t-complex. *EMBO J.* **9**, 2185–2195 (1990).
17. Mehta, A., Kinter, M. T., Sherman, N. E. & Driscoll, D. M. Molecular cloning of apobec-1 complementation factor, a novel RNA-binding protein involved in the editing of apolipoprotein B mRNA. *Mol. Cell. Biol.* **20**, 1846–1854 (2000).
18. Ma, Z. *et al.* Fusion of two novel genes, RBM15 and MKL1, in the t(1;22)(p13;q13) of acute megakaryoblastic leukemia. *Nature Genet.* **28**, 220–221 (2001).
19. Barbouti, A. *et al.* A novel gene, MSI2, encoding a putative RNA-binding protein is recurrently rearranged at disease progression of chronic myeloid leukemia and forms a fusion gene with HOXA9 as a result of the cryptic t(7;17)(p15;q23). *Cancer Res.* **63**, 1202–1206 (2003).
20. Drabkin, H. A. *et al.* DEF-3 (g16/NY-LU-12), an RNA binding protein from the 3p21.3 homozygous deletion region in SCLC. *Oncogene* **18**, 2589–2597 (1999).
21. Ross, J., Lemm, I. & Berberet, B. Overexpression of an mRNA-binding protein in human colorectal cancer. *Oncogene* **20**, 6544–6550 (2001).
22. Jinawath, N., Furukawa, Y. & Nakamura, Y. Identification of NOL8, a nucleolar protein containing an RNA recognition motif (RRM), which is overexpressed in diffuse-type gastric cancer. *Cancer Sci.* **95**, 430–435 (2004).
23. Tsuei, D.-J. *et al.* RBMY, a male germ cell-specific RNA-binding protein, activated in human liver cancers and transforms rodent fibroblasts. *Oncogene* **23**, 5815–5822 (2004).
24. Wedekind, J. E., Dance, G. S. C., Sowden, M. P. & Smith, H. C. Messenger RNA editing in mammals: new members of the APOBEC family seeking roles in the family business. *Trends Genet.* **19**, 207–216 (2003).
25. Martinho, R. G., Kunwar, P. S., Casanova, J. & Lehmann, R. A noncoding RNA is required for the repression of RNA polII-dependent transcription in primordial germ cells. *Curr. Biol.* **14**, 159–165 (2004).
26. Moore, F. L. *et al.* Human pumilio-2 is expressed in embryonic stem cells and germ cells and interacts with DAZ (Deleted in AZoospermia) and DAZ-like proteins. *Proc. Natl Acad. Sci. USA* **100**, 538–543 (2003).
27. Crittenden, S. L. *et al.* A conserved RNA-binding protein controls germline stem cells in *Caenorhabditis elegans*. *Nature* **417**, 660–663 (2002).
28. Burd, C. G. & Dreyfuss, G. Conserved structures and diversity of functions of RNA-binding proteins. *Science* **265**, 615–621 (1994).
29. Yang, X. W., Model, P. & Heintz, N. Homologous recombination based modification in *Escherichia coli* and germline transmission in transgenic mice of a bacterial artificial chromosome. *Nature Biotechnol.* **15**, 859–865 (1997).
30. Henrique, D. *et al.* A digoxigenin labeled RNA probe for Sox9 was detected using an alkaline phosphatase-conjugated anti-digoxigenin antibody. *Nature* **375**, 787–790 (1995).